



Supplement of

Projections of future hydrological drought in a reservoir-regulated region: the roles of climate change and reservoir operation

Shaokun He et al.

Correspondence to: Keping Chen (chenkb@whu.edu.cn) and Yu Gong (ygong@whu.edu.cn)

The copyright of individual parts of the supplement might differ from the article licence.

S1. Hyper-parameter tuning process of LSTM

Since the LSTM models were configured as a three-layer network and the input predictors were identified, the number of hidden nodes, the initial learning rate, and the dropout rate remained to be determined. To this end, a grid-search strategy was used. Specifically, we tested the number of hidden nodes {2, 3, 4, and 8}, the initial learning rate $\{1 \times 10^{-4}, 1 \times 10^{-3}, \text{ and } 5 \times 10^{-3}\}$, the dropout value {0, 0.1, 0.2, and 0.3}. For each configuration, five independent experiments were conducted and their average performance was compared, given the stochastic nature of LSTM simulations. The *NSE* results are summarized in Table S1. Most configurations achieved good performance in daily-scale hydrological simulations, and the differences among repeated experiments were relatively small, suggesting robust model behavior. After screening all configurations, experiment ID 66 was identified as the best performer. Specifically, the selected settings were 4 hidden nodes, an initial learning rate of 1×10^{-4} , and a dropout rate of 0.1 for both the inflow simulation and the operating policy derivation.

At the monthly scale, ID 66 achieved *NSE* values of 0.93 and 0.91 for reservoir inflow and release during the calibration period, respectively, with percent bias (*PBIAS*) values of 3.20% and 3.35%. During the validation period, the *NSE* values were 0.95 and 0.89, with *PBIAS* values of 0.29% and -3.35% , respectively. Overall, these results indicate satisfactory performance across both inflow and release simulations, supporting the subsequent analyses in this study.

S2. Optimization of reservoir operating policies

A multi-objective decision-making problem is formulated for the Ankang reservoir and two objectives are considered: hydropower generation (i.e., total energy generated by the reservoir over the simulation period in units of kWh) and power generation guarantee rate (i.e., the fraction of time periods over the simulation period during which the monthly average power output exceeds the guaranteed power). For medium- and long-term hydropower operations of reservoirs, these two objectives are commonly used to measure operational performance (Chen et al., 2019; Li et al., 2022; Si et al., 2018), which can be expressed by Equations (S1) and (S2).

$$\max f_{THP} = \sum_{t=1}^T \frac{P_t \cdot (\Delta t / 3600)}{Y}, \quad P_t = k \cdot H_t \cdot QG_t \quad (S1)$$

$$\max f_{PGR} = \sum_{t=1}^T \Lambda / T * 100\%, \quad \Lambda = \begin{cases} 0 & \text{if } P_t < P_{gua} \\ 1 & \text{else} \end{cases} \quad (S2)$$

where P_t (kW) is the electric power generated by the reservoir at time t ; k is the efficiency coefficient of the reservoir, which is assumed to be constant over time; H_t (m) is the hydraulic head at time t ; QG_t (m^3/s) is the water release for hydropower generation at time t ; f_{THP} (kW·h) is the total hydropower production (i.e., annual average energy output); Δt (s) is the numerical discretization time step; Y is the total number of years in the simulation periods; T is the total number of time periods; f_{PGR} is the power generation guarantee rate; Λ is a Boolean variable (i.e., 0 or 1), which equals 0 when P_t is less than the guaranteed power and equals 1 otherwise.

Additionally, reservoir operation optimization should satisfy the following constraints:

$$V_{t+1} = V_t + (I_t - O_t) \cdot \Delta t \quad (S3)$$

$$V_{min} \leq V_t \leq V_{max} \quad (S4)$$

$$O_{min} \leq O_t \leq O_{max}, \quad O_t = QG_t + QS_t \quad (S5)$$

$$P_{min} \leq P_t \leq P_{max} \quad (S6)$$

where Equations (S3) - (S5) are the same as Equations (6) – (8) in the main text. QS_t (m^3/s) is the spill flow at time t ; P_{min} (kW) and P_{max} (kW) are the allowable minimum and maximum power outputs, respectively.

We subsequently represent the operating policies with Gaussian radial basis functions (RBFs) due to their reported positive scalability with respect to the state-decision space (Yang et al., 2020; Quinn et al., 2017). The RBF-based policy representation is expressed in Equation (S7), where u_t is the policy-designated reservoir release at time t (normalized to $[0, 1]$), $(X_t)_m$ is the value of the m th of M time-varying inputs at time t (normalized to $[0, 1]$), and w_k , $c_{k,m}$, and b_k are the weights, centers, and radii of RBFs, respectively.

$$u_t = \sum_{k=1}^K w_k \exp \left[-\sum_{m=1}^M \frac{((X_t)_m - c_{k,m})^2}{b_k} \right] \quad (S7)$$

where $w_k \in [0,1]$ with $\sum_{k=1}^K w_k = 1$, $c_{k,m} \in [-1,1]$, and $b_{k,m} \in (0,1]$. We modeled reservoir releases using three inputs: current reservoir storage, current reservoir inflow, and time of year, as suggested by Yang et al. (2017) for this reservoir system. Notably, the final true release at time t may not always be equal to the unnormalized policy-designated release at time t due to physical release constraints. If there is insufficient reservoir storage capacity to allow a release of only the unnormalized magnitude of u_t , the excess is spilled, and if there is less water than the unnormalized u_t , only the available water is released.

Finally, we used the nondominated sorting genetic algorithm II (NSGA-II) (Deb et al., 2002) to optimize the policy parameters. The population size and number of generations were set to 100 and 1000, respectively. The resulting Pareto front π_θ^* is shown in Figure 10 in the main manuscript.

Table S1. The average *Nash-Sutcliffe (NSE)* performance of LSTM in the daily hydrological simulation with different hyper-parameter combinations.

Experiment ID	Hidden_size	End_lr	Hidden_channel	dropout	Calibration period (1993-2014)		Validation period (2015-2020)	
					Inflow	Release	Inflow	Release
1	8	0.005	8	0	0.864	0.802	0.736	0.651
2	8	0.001	8	0	0.862	0.797	0.733	0.649
3	8	1.00E-04	8	0	0.862	0.804	0.733	0.64
4	8	0.005	8	0.1	0.857	0.799	0.74	0.659
5	8	0.001	8	0.1	0.855	0.792	0.736	0.656
6	8	1.00E-04	8	0.1	0.853	0.785	0.735	0.652
7	8	0.005	8	0.2	0.853	0.79	0.741	0.659
8	8	0.001	8	0.2	0.852	0.785	0.741	0.657
9	8	1.00E-04	8	0.2	0.853	0.783	0.744	0.657
10	8	0.005	8	0.3	0.851	0.789	0.747	0.661
11	8	0.001	8	0.3	0.851	0.784	0.746	0.658
12	8	1.00E-04	8	0.3	0.847	0.782	0.741	0.656
13	8	0.005	4	0	0.856	0.805	0.729	0.646
14	8	0.001	4	0	0.853	0.8	0.72	0.641
15	8	1.00E-04	4	0	0.854	0.8	0.726	0.648
16	8	0.005	4	0.1	0.854	0.794	0.739	0.669
17	8	0.001	4	0.1	0.853	0.788	0.739	0.676
18	8	1.00E-04	4	0.1	0.852	0.791	0.736	0.666
19	8	0.005	4	0.2	0.849	0.79	0.743	0.678
20	8	0.001	4	0.2	0.849	0.792	0.744	0.67
21	8	1.00E-04	4	0.2	0.847	0.792	0.742	0.668
22	8	0.005	4	0.3	0.833	0.756	0.735	0.684
23	8	0.001	4	0.3	0.835	0.777	0.742	0.673
24	8	1.00E-04	4	0.3	0.836	0.772	0.736	0.675
25	8	0.005	3	0	0.849	0.794	0.711	0.638
26	8	0.001	3	0	0.847	0.795	0.706	0.62
27	8	1.00E-04	3	0	0.843	0.789	0.703	0.625
28	8	0.005	3	0.1	0.852	0.799	0.738	0.673
29	8	0.001	3	0.1	0.852	0.794	0.737	0.671
30	8	1.00E-04	3	0.1	0.851	0.792	0.737	0.663
31	8	0.005	3	0.2	0.843	0.787	0.74	0.679
32	8	0.001	3	0.2	0.841	0.783	0.735	0.678
33	8	1.00E-04	3	0.2	0.837	0.767	0.734	0.681
34	8	0.005	3	0.3	0.833	0.77	0.74	0.685
35	8	0.001	3	0.3	0.828	0.761	0.73	0.678
36	8	1.00E-04	3	0.3	0.827	0.756	0.735	0.683
37	8	0.005	2	0	0.85	0.798	0.714	0.639
38	8	0.001	2	0	0.849	0.8	0.712	0.619
39	8	1.00E-04	2	0	0.848	0.8	0.709	0.617
40	8	0.005	2	0.1	0.841	0.748	0.726	0.682

41	8	0.001	2	0.1	0.844	0.78	0.724	0.663
42	8	1.00E-04	2	0.1	0.844	0.779	0.727	0.657
43	8	0.005	2	0.2	0.831	0.763	0.733	0.68
44	8	0.001	2	0.2	0.827	0.755	0.731	0.676
45	8	1.00E-04	2	0.2	0.828	0.758	0.73	0.677
46	8	0.005	2	0.3	0.809	0.764	0.725	0.67
47	8	0.001	2	0.3	0.808	0.758	0.73	0.67
48	8	1.00E-04	2	0.3	0.809	0.756	0.73	0.669
49	4	0.005	8	0	0.862	0.8	0.737	0.661
50	4	0.001	8	0	0.864	0.806	0.736	0.655
51	4	1.00E-04	8	0	0.864	0.804	0.734	0.653
52	4	0.005	8	0.1	0.852	0.798	0.754	0.658
53	4	0.001	8	0.1	0.856	0.802	0.742	0.649
54	4	1.00E-04	8	0.1	0.855	0.795	0.741	0.654
55	4	0.005	8	0.2	0.855	0.795	0.74	0.661
56	4	0.001	8	0.2	0.853	0.792	0.747	0.658
57	4	1.00E-04	8	0.2	0.855	0.798	0.751	0.65
58	4	0.005	8	0.3	0.845	0.784	0.748	0.661
59	4	0.001	8	0.3	0.844	0.786	0.743	0.654
60	4	1.00E-04	8	0.3	0.845	0.788	0.746	0.649
61	4	0.005	4	0	0.862	0.799	0.73	0.649
62	4	0.001	4	0	0.862	0.799	0.731	0.642
63	4	1.00E-04	4	0	0.861	0.802	0.725	0.637
64	4	0.005	4	0.1	0.854	0.8	0.742	0.657
65	4	0.001	4	0.1	0.856	0.802	0.744	0.649
66	4	1.00E-04	4	0.1	0.851	0.793	0.74	0.65
67	4	0.005	4	0.2	0.847	0.774	0.739	0.692
68	4	0.001	4	0.2	0.844	0.781	0.742	0.661
69	4	1.00E-04	4	0.2	0.846	0.787	0.742	0.663
70	4	0.005	4	0.3	0.835	0.777	0.743	0.665
71	4	0.001	4	0.3	0.835	0.78	0.735	0.661
72	4	1.00E-04	4	0.3	0.833	0.776	0.742	0.663
73	4	0.005	3	0	0.848	0.793	0.698	0.63
74	4	0.001	3	0	0.85	0.796	0.708	0.621
75	4	1.00E-04	3	0	0.85	0.793	0.707	0.624
76	4	0.005	3	0.1	0.849	0.796	0.74	0.67
77	4	0.001	3	0.1	0.848	0.797	0.733	0.658
78	4	1.00E-04	3	0.1	0.847	0.793	0.734	0.656
79	4	0.005	3	0.2	0.835	0.764	0.732	0.677
80	4	0.001	3	0.2	0.836	0.78	0.737	0.669
81	4	1.00E-04	3	0.2	0.834	0.773	0.737	0.668
82	4	0.005	3	0.3	0.825	0.765	0.734	0.673
83	4	0.001	3	0.3	0.822	0.764	0.731	0.67
84	4	1.00E-04	3	0.3	0.822	0.766	0.734	0.668
85	4	0.005	2	0	0.847	0.802	0.708	0.627

86	4	0.001	2	0	0.846	0.801	0.705	0.619
87	4	1.00E-04	2	0	0.845	0.8	0.704	0.622
88	4	0.005	2	0.1	0.843	0.775	0.735	0.656
89	4	0.001	2	0.1	0.842	0.781	0.732	0.658
90	4	1.00E-04	2	0.1	0.845	0.788	0.733	0.65
91	4	0.005	2	0.2	0.831	0.767	0.734	0.669
92	4	0.001	2	0.2	0.827	0.762	0.73	0.66
93	4	1.00E-04	2	0.2	0.825	0.766	0.73	0.658
94	4	0.005	2	0.3	0.803	0.738	0.725	0.671
95	4	0.001	2	0.3	0.801	0.738	0.722	0.666
96	4	1.00E-04	2	0.3	0.799	0.733	0.722	0.663
97	3	0.005	8	0	0.866	0.803	0.744	0.653
98	3	0.001	8	0	0.866	0.806	0.737	0.641
99	3	1.00E-04	8	0	0.865	0.806	0.735	0.64
100	3	0.005	8	0.1	0.858	0.803	0.746	0.667
101	3	0.001	8	0.1	0.856	0.8	0.748	0.669
102	3	1.00E-04	8	0.1	0.853	0.791	0.743	0.656
103	3	0.005	8	0.2	0.856	0.797	0.75	0.667
104	3	0.001	8	0.2	0.852	0.795	0.748	0.659
105	3	1.00E-04	8	0.2	0.855	0.799	0.748	0.654
106	3	0.005	8	0.3	0.843	0.781	0.748	0.66
107	3	0.001	8	0.3	0.847	0.79	0.749	0.648
108	3	1.00E-04	8	0.3	0.847	0.794	0.749	0.651
109	3	0.005	4	0	0.859	0.794	0.737	0.656
110	3	0.001	4	0	0.861	0.803	0.73	0.644
111	3	1.00E-04	4	0	0.862	0.806	0.732	0.638
112	3	0.005	4	0.1	0.855	0.801	0.749	0.667
113	3	0.001	4	0.1	0.851	0.796	0.746	0.669
114	3	1.00E-04	4	0.1	0.855	0.801	0.746	0.662
115	3	0.005	4	0.2	0.848	0.792	0.745	0.669
116	3	0.001	4	0.2	0.846	0.794	0.75	0.667
117	3	1.00E-04	4	0.2	0.845	0.791	0.746	0.669
118	3	0.005	4	0.3	0.835	0.78	0.744	0.662
119	3	0.001	4	0.3	0.832	0.779	0.743	0.67
120	3	1.00E-04	4	0.3	0.828	0.777	0.736	0.668
121	3	0.005	3	0	0.857	0.796	0.727	0.66
122	3	0.001	3	0	0.859	0.805	0.725	0.641
123	3	1.00E-04	3	0	0.856	0.798	0.727	0.641
124	3	0.005	3	0.1	0.851	0.797	0.747	0.663
125	3	0.001	3	0.1	0.849	0.788	0.745	0.666
126	3	1.00E-04	3	0.1	0.851	0.801	0.743	0.66
127	3	0.005	3	0.2	0.843	0.787	0.749	0.67
128	3	0.001	3	0.2	0.841	0.788	0.748	0.663
129	3	1.00E-04	3	0.2	0.842	0.792	0.747	0.659
130	3	0.005	3	0.3	0.825	0.766	0.743	0.666

131	3	0.001	3	0.3	0.825	0.77	0.74	0.65
132	3	1.00E-04	3	0.3	0.828	0.776	0.742	0.655
133	3	0.005	2	0	0.851	0.797	0.716	0.63
134	3	0.001	2	0	0.846	0.796	0.708	0.618
135	3	1.00E-04	2	0	0.848	0.794	0.712	0.628
136	3	0.005	2	0.1	0.848	0.781	0.739	0.664
137	3	0.001	2	0.1	0.846	0.783	0.738	0.658
138	3	1.00E-04	2	0.1	0.846	0.784	0.737	0.667
139	3	0.005	2	0.2	0.834	0.78	0.744	0.662
140	3	0.001	2	0.2	0.83	0.772	0.737	0.661
141	3	1.00E-04	2	0.2	0.83	0.765	0.734	0.66
142	3	0.005	2	0.3	0.807	0.743	0.731	0.666
143	3	0.001	2	0.3	0.806	0.742	0.726	0.667
144	3	1.00E-04	2	0.3	0.802	0.736	0.723	0.662
145	2	0.005	8	0	0.862	0.798	0.741	0.659
146	2	0.001	8	0	0.864	0.805	0.734	0.638
147	2	1.00E-04	8	0	0.863	0.802	0.739	0.642
148	2	0.005	8	0.1	0.857	0.802	0.748	0.65
149	2	0.001	8	0.1	0.858	0.8	0.748	0.651
150	2	1.00E-04	8	0.1	0.855	0.799	0.746	0.657
151	2	0.005	8	0.2	0.853	0.79	0.748	0.659
152	2	0.001	8	0.2	0.855	0.796	0.75	0.655
153	2	1.00E-04	8	0.2	0.852	0.799	0.746	0.653
154	2	0.005	8	0.3	0.846	0.784	0.748	0.645
155	2	0.001	8	0.3	0.843	0.782	0.75	0.636
156	2	1.00E-04	8	0.3	0.847	0.788	0.749	0.638
157	2	0.005	4	0	0.861	0.8	0.732	0.654
158	2	0.001	4	0	0.861	0.806	0.732	0.649
159	2	1.00E-04	4	0	0.86	0.805	0.729	0.643
160	2	0.005	4	0.1	0.85	0.789	0.741	0.664
161	2	0.001	4	0.1	0.855	0.804	0.74	0.66
162	2	1.00E-04	4	0.1	0.853	0.8	0.741	0.66
163	2	0.005	4	0.2	0.842	0.786	0.74	0.66
164	2	0.001	4	0.2	0.839	0.772	0.737	0.649
165	2	1.00E-04	4	0.2	0.844	0.791	0.744	0.644
166	2	0.005	4	0.3	0.832	0.778	0.742	0.656
167	2	0.001	4	0.3	0.829	0.773	0.736	0.64
168	2	1.00E-04	4	0.3	0.829	0.775	0.737	0.653
169	2	0.005	3	0	0.857	0.806	0.716	0.625
170	2	0.001	3	0	0.852	0.8	0.712	0.623
171	2	1.00E-04	3	0	0.851	0.801	0.707	0.613
172	2	0.005	3	0.1	0.849	0.801	0.756	0.661
173	2	0.001	3	0.1	0.855	0.801	0.741	0.655
174	2	1.00E-04	3	0.1	0.855	0.8	0.742	0.66
175	2	0.005	3	0.2	0.841	0.785	0.752	0.665

176	2	0.001	3	0.2	0.838	0.785	0.744	0.661
177	2	1.00E-04	3	0.2	0.841	0.785	0.746	0.665
178	2	0.005	3	0.3	0.819	0.767	0.737	0.654
179	2	0.001	3	0.3	0.819	0.767	0.733	0.647
180	2	1.00E-04	3	0.3	0.819	0.766	0.74	0.652
181	2	0.005	2	0	0.844	0.799	0.693	0.615
182	2	0.001	2	0	0.846	0.799	0.706	0.618
183	2	1.00E-04	2	0	0.846	0.799	0.705	0.615
184	2	0.005	2	0.1	0.838	0.783	0.723	0.663
185	2	0.001	2	0.1	0.841	0.792	0.72	0.649
186	2	1.00E-04	2	0.1	0.837	0.789	0.717	0.643
187	2	0.005	2	0.2	0.824	0.768	0.718	0.66
188	2	0.001	2	0.2	0.821	0.772	0.719	0.652
189	2	1.00E-04	2	0.2	0.822	0.773	0.723	0.659
190	2	0.005	2	0.3	0.803	0.755	0.715	0.652
191	2	0.001	2	0.3	0.793	0.741	0.707	0.649
192	2	1.00E-04	2	0.3	0.798	0.749	0.713	0.649

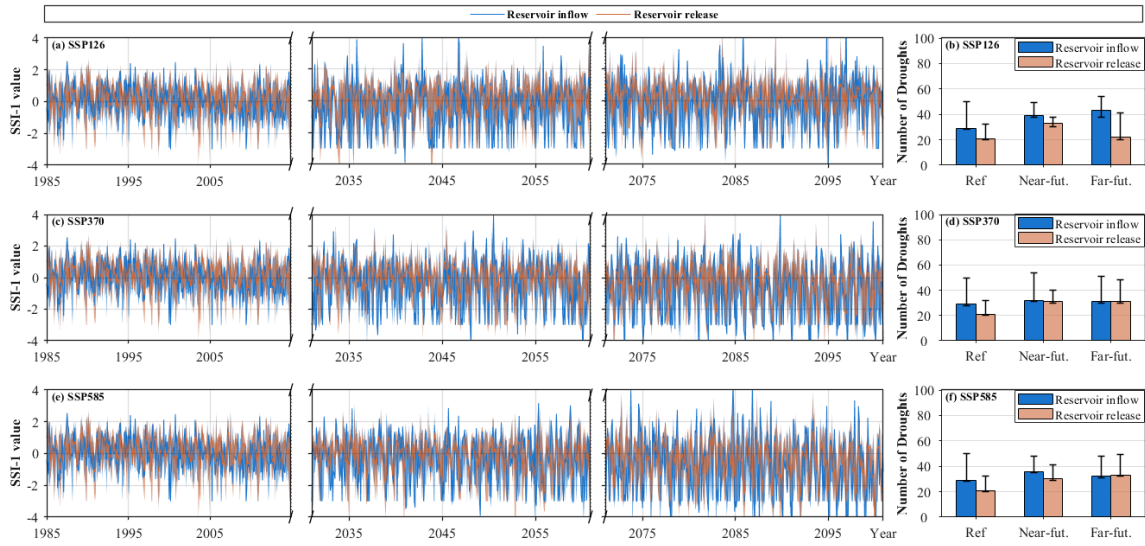


Figure S1. Hydrological drought SSI-1 for reference and future periods over the UHRB. (a) Time series of SSI-1 associated with reservoir inflow and release for the low-emission SSP126 scenario. Blue and orange intervals indicate their uncertainties, respectively. (b) Number of drought events for the reference period (1985–2014), near-future period (2031–2060), and far-future period (2071–2100). Colored bars are ensemble means and error bars represent the estimated difference in the number of drought events among the five GCMs. Panels (c,d) and (e,f) are the same as panels (a,b), but for the medium-emission SSP370 and high-emission SSP585 scenarios, respectively.

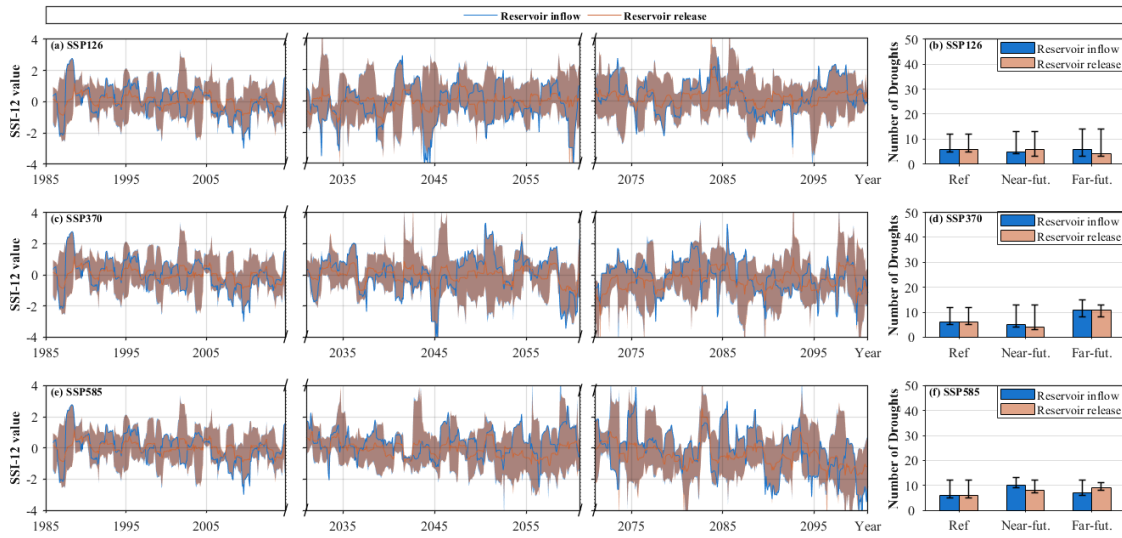


Figure S2. Hydrological drought SSI-12 for reference and future periods over the UHRB. (a) Time series of SSI-12 associated with reservoir inflow and release for the low-emission SSP126 scenario. Blue and orange intervals indicate their uncertainties, respectively. (b) Number of drought events for the reference period (1985–2014), near-future period (2031–2060), and far-future period (2071–2100). Colored bars are ensemble means and error bars represent the estimated difference in the number of drought events among the five GCMs. Panels (c,d) and (e,f) are the same as panels (a,b), but for the medium-emission SSP370 and high-emission SSP585 scenarios, respectively.

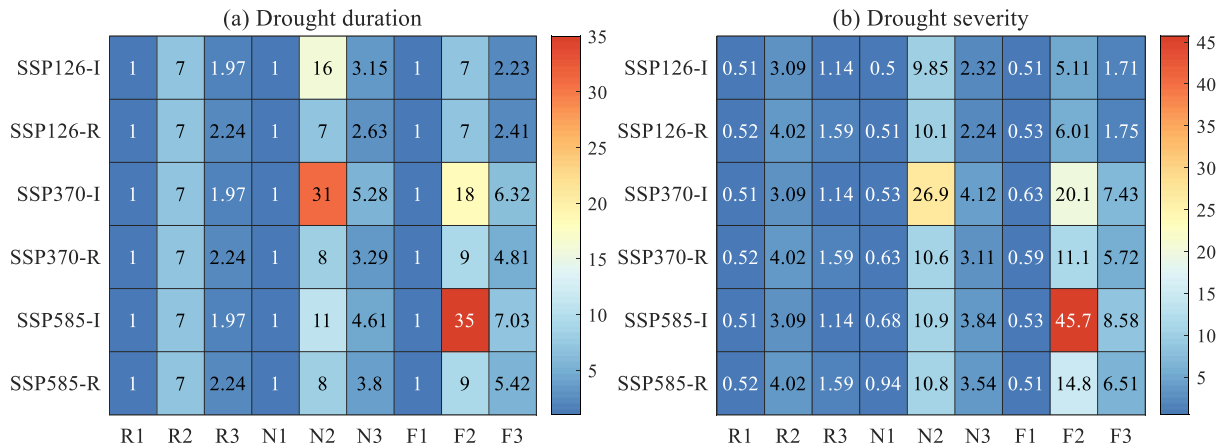


Figure S3. Heat map representation of (a) drought duration and (b) drought severity for the GCM-averaged SSI-1 series. The symbols R1, R2 and R3 indicate the minimum, maximum, and mean values during the reference period (1985–2014). N1, N2 and N3 are the same, but for the near-future period (2031–2060). F1, F2, and F3 are for the far-future period (2071–2100). Additionally, SSP126-I and SSP126-R are associated with reservoir inflow and release in the SSP126 scenario, SSP370-I and SSP370-R with the SSP370 scenario, and SSP585-I and SSP585-R with the SSP585 scenario.

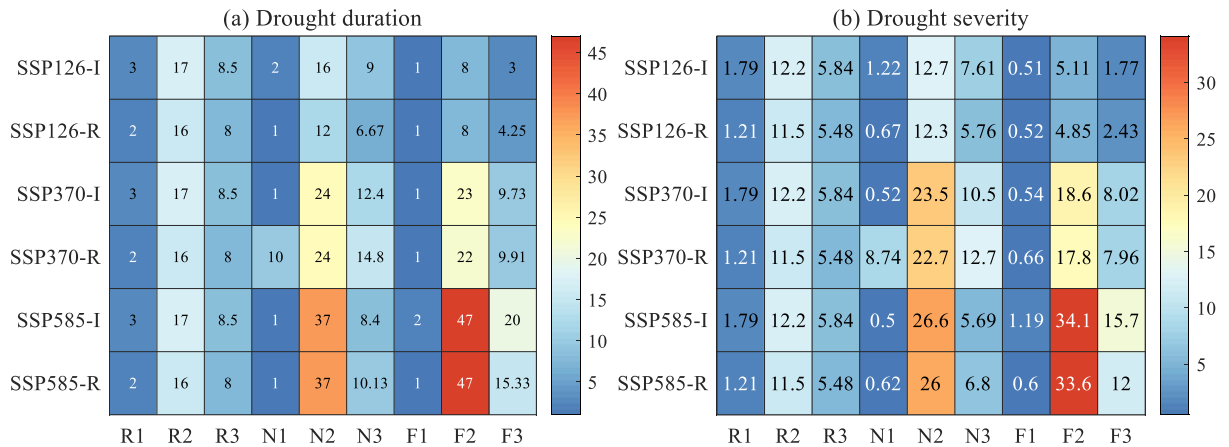


Figure S4. Heat map representation of (a) drought duration and (b) drought severity for the GCM-averaged SSI-12 series. The symbols R1, R2 and R3 indicate the minimum, maximum, and mean values during the reference period (1985–2014). N1, N2 and N3 are the same, but for the near-future period (2031–2060). F1, F2, and F3 are for the far-future period (2071–2100). Additionally, SSP126-I and SSP126-R are associated with reservoir inflow and release in the SSP126 scenario, SSP370-I and SSP370-R with the SSP370 scenario, and SSP585-I and SSP585-R with the SSP585 scenario.

Acronyms and Notation

For ease of reading, all important and notations in the main text are summarized below.

Acronyms

UHRB	Upper Hanjiang River Basin
SSI	Standard Streamflow Index
LSTM	Long and Short-Term Memory
GCM	Global Climate Model
SSP	Shared Socioeconomic Pathway
ML	Machine Learning
CMA	China Meteorological Administration
ISIMIP3b	Inter-sectoral Impact Model Intercomparison Project 3b
NSGA-III	Nondominated sorting genetic algorithm version III
FDC	Flow Duration Curve
NSE	Nash–Sutcliffe efficiency

Notation for key variables

f	Operating objective vector
π_{θ}^*	Optimal operating policies
w^H	Historical climate conditions
V	Reservoir storage
I	Reservoir inflow
O	Reservoir release
D	Duration of hydrological drought
S	Severity of hydrological drought

References

- Chen, X., Xu, B., Zheng, Y., and Zhang, C.: Nexus of water, energy and ecosystems in the upper Mekong River: A system analysis of phosphorus transport through cascade reservoirs, *Sci Total Environ*, 671, 1179-1191, 10.1016/j.scitotenv.2019.03.324, 2019.
- Deb, K., Pratap, A., Agarwal, S., and Meyarivan, T.: A fast and elitist multiobjective genetic algorithm: NSGA-II, *Ieee T Evolut Comput*, 6, 182-197, 10.1109/4235.996017, 2002.
- Li, X., Liu, P., Wang, Y., Yang, Z., Gong, Y., An, R., Huang, K., and Wen, Y.: Derivation of operating rule curves for cascade hydropower reservoirs considering the spot market: A case study of the China's Qing River cascade-reservoir system, *Renewable Energy*, 182, 1028-1038, 10.1016/j.renene.2021.11.013, 2022.
- Quinn, J. D., Reed, P. M., Giuliani, M., and Castelletti, A.: Rival framings: A framework for discovering how problem formulation uncertainties shape risk management trade - offs in water resources systems, *Water Resour Res*, 53, 7208-7233, 10.1002/2017wr020524, 2017.
- Si, Y., Li, X., Yin, D., Liu, R., Wei, J., Huang, Y., Li, T., Liu, J., Gu, S., and Wang, G.: Evaluating and optimizing the operation of the hydropower system in the Upper Yellow River: A general LINGO-based integrated framework, *Plos One*, 13, e0191483, 10.1371/journal.pone.0191483, 2018.
- Yang, G., Guo, S. L., Liu, P., and Block, P.: Integration and evaluation of forecast-informed multiobjective reservoir operations, *J Water Res Plan Man*, 146, 04020038, 10.1061/(Asce)Wr.1943-5452.0001229, 2020.
- Yang, G., Guo, S. L., Liu, P., Li, L. P., and Xu, C. Y.: Multiobjective reservoir operating rules based on cascade reservoir input variable selection method, *Water Resour Res*, 53, 3446-3463, 10.1002/2016wr020301, 2017.